Spontaneous emission of two quantum dots in a single-mode cavity*

Qiu Liu(邱 柳), Zhang Ke(张 珂), and Li Zhi-Yuan(李志远)†

Laboratory of Optical Physics, Institute of Physics, Chinese Academy of Sciences, Beijing 100190, *China*

(Received 1 March 2013; revised manuscript received 2 April 2013)

The spontaneous emission spectrum from two quantum dots (QDs) that are strongly coupled with a single-mode nanocavity is investigated using rigorous numerical calculations and simple analytical solutions of quantum dynamics. The emission spectra both from the side and along the axis of the cavity are considered. Modification of two parameters, the coupling strength and the detuning between the transition frequencies of the two quantum dots, allows us to efficiently control the shape of the spontaneous emission spectrum. Different profiles and their physical origins can be well understood in the dressed-state picture for the light–QD interaction in the on-resonance and off-resonance situations. In the on-resonance situation, the emission spectra exhibit symmetric features, and they are not altered by the asymmetry in the coupling parameters. The axis spectra show two emission peaks while the side spectra have three emission peaks. In the off-resonance situation, the emission spectra always show an asymmetrical three-peak feature. When the two QDs have different decay parameters, singular features (a peak or a dip) can take place at the frequency of the cavity mode, and this is attributed to the unbalanced process of the emission and absorption of a single photon.

Keywords: spontaneous emission, quantum dot, single-mode cavity

PACS: 42.50.Pq, 03.65.Yz, 78.67.Hc **DOI:** 10.1088/1674-1056/22/9/094207

1. Introduction

Recently, cavity quantum electrodynamics (QED) has been actively pursued for its potential insight into the fundamental problems of light-matter interaction.[1,2] Most of the schemes that involve cavities, which contains trapped qubits, have shown promise towards the realization of quantum information storage and processing.[3–5] In accordance with a general desire to control quantum systems in all solid platforms for practical applications and ease of integration, considerable attention has turned to the cavity QED in photonic crystals (PCs),[6–8] which are also called photonic band gap (PBG) materials. A point defect in PCs defines a PBG cavity, as any photon injected into that site cannot propagate laterally away from the defect. In this way, the PBG cavities can constitute extremely good cavities with superb photonic confinement (low loss and ultra small mode volume) and strong light-matter coupling for an embedded quantum system. The photonic local density of states,[9,10] which is a key physical function in PCs, is directly connected to the coupling strength with the quantum emitter, for example, a quantum dot (QD), which is often considered to be a two-level atom-like emitter.[11,12] The coherent interaction between QD excitons and cavity modes in PCs has raised great interest in a lot of areas, such as giant optical nonlinearity induced by the Purcell effect,[13,14] a one-atom laser in the strong coupling limit,[15–18] modified spontaneous emission,[19–25] and QDs embedded in PC waveguides.[26–29] The dynamical behavior of entangled states, which are an essential source for quantum computing and quantum-information processes, has been investigated by considering a model consisting of two or more QDs trapped in PBG cavities.[30–37]

In this paper, we consider the spontaneous emission spectra of two QDs that are strongly coupled with a single-mode cavity field in thermal equilibrium. Due to the great distance between the two QDs, we neglect their dipole–dipole interactions. Our theory is rigorous, yet it is also very intuitive and clear, so it will be immediately helpful to experimentalists working in this field. In our cavity QED model, two important parameters are used to characterize the system: the QD-cavity coupling constant and the detuning between the transition frequencies of the two QDs. The axis and side spontaneous emission spectra will be analyzed from different aspects of these two parameters. On one hand, we consider two general cases: the on-resonance case and the off-resonance case. In the on-resonance case, where the transition frequencies of the two QDs are equal to each other, the influence of the coupling strength parameters on the emission spectra has been studied. The Rabi oscillation leads to a symmetrical splitting of the emission spectra and the large coupling strength results in a wider split. The intensity change of the peaks with respect to the coupling constants is also investigated. In the off-resonance case, where the detuning between the two transition frequencies is not zero, the axis and side emission spectra both have three peaks, and they are no longer completely symmetric. The detuning parameter dominates the distribution of population. By exchanging the two transition frequencies, the new spectrum is just the mirror inversion of the old one. On the other hand, when the two decay parameters are not

*Project supported by the National Basic Research Foundation of China (Grant No. 2011CB922002).

†Corresponding author. E-mail: lizy@aphy.iphy.ac.cn

© 2013 Chinese Physical Society and IOP Publishing Ltd

equal to each other, a singular feature (a peak or a dip) will appear at the frequency of the cavity mode in the axis spectrum. This phenomenon is attributed to the unbalanced process of the emission and absorption of a single photon by the QD and the PBG cavity.

This article is organized as follows. In Section 2, we derive the quantum mechanical equations governing the axis and side spontaneous spectrum of two QDs embedded in a PBG cavity. In Section 3, we make a detailed analysis of three cases of light–QD interaction. Both numerical calculations and analytical formalisms are used to sharpen and deepen our understanding of the quantum dynamics of the coupled QD–photon system. In Section 4, we make a brief conclusion.

2. Model and formalism

The QD-cavity system considered in this paper is schematically illustrated in Fig. 1. The two QDs (A and B) are located on the axis at two antinodes of the standing-wave cavity mode that supports sufficiently strong coupling strength. Assuming that the distance between A and B is long enough, the dipole–dipole interaction can be reasonably neglected. For simplicity, we also assume that the system temperature is 0°C, where the dephasing rate can be ignored. We assume that one of the two QDs is initially prepared in an excited state, while the other is in the ground state, and the cavity is in the vacuum state.

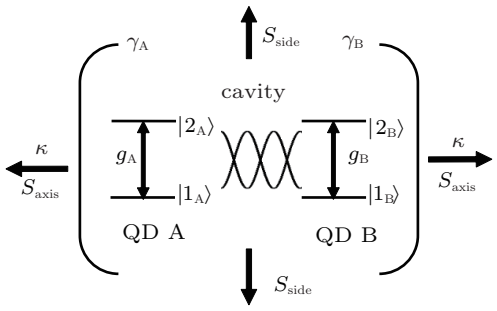


Fig. 1. Schematic diagram of the coupling between two QDs and a single-mode cavity. Photons can be emitted out from the sides of the cavity and through the axis direction.

In a frame rotating with the laser frequency, under the rotating wave approximation (RWA), the Hamiltonian could be written as

$$H = \sum_{j=\mathrm{A,B}} \left[\hbar\Delta_{j\mathrm{c}}\sigma_{22}^{j} + \mathrm{i}\hbar g_j\left(a^{\dagger}\sigma_{-}^{j} - \sigma_{+}^{j}a\right)\right], \tag{1}$$

where $a^{\dagger}$ and a are the creation and annihilation operators for the cavity mode, σ^j ($j = \mathrm{A,B}$) are Pauli pseudo-spin operators for the two QDs, $\Delta_{j\mathrm{c}} = \omega_j - \omega_{\mathrm{c}}$ is the detuning between the transition frequency of the QDs (ω_j) and the resonant frequency of the cavity mode (ω_{c}), and g_j are the coupling constants between the QDs and the cavity mode. These parameters refer to the cavity QED parameters. Let $\mathrm{L}\rho$ represent all the dissipative terms, we have

$$\begin{aligned}\mathrm{L}\rho \;=\; & \sum_{j=\mathrm{A,B}}\left[\frac{\gamma_j}{2}\left(2\sigma_{-}^{j}\rho\sigma_{+}^{j} - \sigma_{+}^{j}\sigma_{-}^{j}\rho - \rho\sigma_{+}^{j}\sigma_{-}^{j}\right)\right. \\ & \left. + \kappa\left(2a\rho a^{\dagger} - a^{\dagger}a\rho - \rho a^{\dagger}a\right)\right],\end{aligned} \tag{2}$$

where γ_j characterizes the spontaneous emission rate of the QDs. The cavity field is damped at the rate κ, which is caused by the extraneous coupling of the cavity mode to the external reservoirs or possible leakage of light from the PBG nanocavity.

Assume that QD A is prepared in the excited state at the initial time $t = 0$ (namely, $\left\langle\sigma_{22}^{\mathrm{A}}(0)\right\rangle = 1$), and define the detuning between the cavity-mode frequency and the average transition frequency of the two QDs as $\Delta_{\mathrm{c}} = (\omega_{\mathrm{A}} + \omega_{\mathrm{B}})/2 - \omega_{\mathrm{c}}$. The solution and discussion of the dynamics of the Hamiltonian are restricted to the subspace containing zero and one excitations. We can thus write the state vector of the system at time t as

$$\begin{aligned}|\Psi(t)\rangle \;&=\; |\psi_0(t)\rangle + |\psi_1(t)\rangle,\\ |\psi_0(t)\rangle \;&=\; |1_{\mathrm{A}}\rangle|1_{\mathrm{B}}\rangle|0\rangle,\\ |\psi_1(t)\rangle \;&=\; a(t)|2_{\mathrm{A}}\rangle|1_{\mathrm{B}}\rangle|0\rangle + b(t)|1_{\mathrm{A}}\rangle|2_{\mathrm{B}}\rangle|0\rangle\\ &\quad + c(t)|1_{\mathrm{A}}\rangle|1_{\mathrm{B}}\rangle|1\rangle.\end{aligned} \tag{3}$$

Here $|1_j\rangle$ and $|2_j\rangle$ are the ground and excited states of QD j, and $|0\rangle$ and $|1\rangle$ are the vacuum and one photon state of the cavity mode. The zero-excitation component $|\psi_0(t)\rangle$ is invariant under the action of the Hamiltonian, so we only need to consider the dynamics of the single-excitation component $|\psi_1(t)\rangle$.

The initial conditions that QD A is prepared in the excited state, QD B is in the ground state, and the cavity is in the vacuum state require that the initial state is

$$|\psi_1(0)\rangle = |2_{\mathrm{A}}\rangle|1_{\mathrm{B}}\rangle|0\rangle. \tag{4}$$

Then, the coefficients of $|\psi_1(0)\rangle$ are $a(0) = 1$ and $b(0) = c(0) = 0$. The time evolution of the general one-excitation state given by Eq. (3) can be calculated exactly from the Schrödinger equation with a non-Hermitian Hamiltonian as

$$\begin{aligned}H_{\mathrm{C}} \;=\; & \sum_{j=A,B}\left[\hbar\Delta_{j\mathrm{c}}\sigma_{22}^{j} + \mathrm{i}\hbar g_j\left(a^{\dagger}\sigma_{-}^{j} - \sigma_{+}^{j}a\right) - \mathrm{i}\hbar\frac{\gamma_j}{2}\sigma_{22}^{j}\right]\\ & - \mathrm{i}\hbar\kappa a^{\dagger}a.\end{aligned}$$

The results are

$$\begin{aligned}\dot{a}(t) &= -\kappa_{\mathrm{a}}a(t) - g_{\mathrm{A}}c(t),\\ \dot{b}(t) &= -\kappa_{\mathrm{b}}b(t) - g_{\mathrm{B}}c(t),\\ \dot{c}(t) &= -\kappa_{\mathrm{c}}c(t) + g_{\mathrm{A}}a(t) + g_{\mathrm{B}}b(t).\end{aligned} \tag{5}$$

The parameters are defined as

$$\kappa_{\mathrm{c}} = \kappa,$$

$$\kappa_{\rm a} = {\rm i}\,(\Delta_{\rm c} + \omega_{\rm AB}) + \frac{\gamma_{\rm A}}{2},$$
$$\kappa_{\rm b} = {\rm i}\,(\Delta_{\rm c} - \omega_{\rm AB}) + \frac{\gamma_{\rm B}}{2},$$

where $\omega_{\rm AB} = (\omega_{\rm A} - \omega_{\rm B})/2$. In order to solve the above equation set, we assume a trial solution as $a(t) = A\,{\rm e}^{xt}$, $b(t) = B\,{\rm e}^{xt}$, and $c(t) = C\,{\rm e}^{xt}$. Inserting the trial solution into Eq. (5) leads to a set of linear equations of a 3×3 eigensystem

$$\begin{pmatrix} -\kappa_{\rm a} & 0 & -g_{\rm A} \\ 0 & -\kappa_{\rm b} & -g_{\rm B} \\ g_{\rm A} & g_{\rm B} & -\kappa_{\rm c} \end{pmatrix} \begin{pmatrix} A \\ B \\ C \end{pmatrix} = x \begin{pmatrix} A \\ B \\ C \end{pmatrix}, \tag{6}$$

where x is the eigenvalue. The solution of Eq. (6) is straightforward and yields three roots x_n. As a result, each trial function is a harmonic wave function. The general solution of dynamics can be described by these wavefunctions. The coefficient $a(t)$ for the one-excitation state $|2_{\rm A}\rangle\,|1_{\rm B}\rangle\,|0\rangle$ is given by

$$a(t) = \sum_{n=1}^{3} A_n\,{\rm e}^{x_n t}, \tag{7}$$

and the coefficients of other one-excitation states can be derived from $a(t)$ by going back to Eq. (5). Other quantities can be readily calculated from $a(t)$ by considering Eq. (5). Finally, the amplitude of each state is given by

$$\begin{aligned} a(t) &= \sum_{n=1}^{3} A_n\,{\rm e}^{x_n t}, \\ b(t) &= -\sum_{n=1}^{3} \frac{(x_n + \kappa_{\rm a})\,(x_n + \kappa_{\rm b}) + g_{\rm A}^2}{g_{\rm A} g_{\rm B}} A_n\,{\rm e}^{x_n t}, \\ c(t) &= -\sum_{n=1}^{3} \frac{x_n + \kappa_{\rm a}}{g_{\rm A}} A_n\,{\rm e}^{x_n t}. \end{aligned} \tag{8}$$

By using the initial condition (4) of the three one-excitation states, we can work out the numerical value of A_n by straightforward calculations in Ref. [31]. Equation (8) contains an implicit dependence on the coupling constants, the transition frequencies, and the decay parameters of the QD-cavity structure. Since these parameters determine the structure of the emission spectra, we will carry out a detailed study of the spectra for various values of g_j, $\omega_{\rm AB}$, and γ_j in Section 3.

According to the quantum regression theorem,[1] one can find from Eq. (8) that the spontaneous emission spectrum of this system includes two parts in the long-time limit. One is the spectrum from the sides of the cavity, which is determined from the autocorrelation of the atomic dipole amplitude and reads

$$\begin{aligned} S_{\rm side} &= \frac{\gamma_{\rm A}}{2\pi} \left| \int_0^\infty {\rm d}t\,{\rm e}^{{\rm i}\omega t} a(t) \right|^2 + \frac{\gamma_{\rm B}}{2\pi} \left| \int_0^\infty {\rm d}t\,{\rm e}^{{\rm i}\omega t} b(t) \right|^2 \\ &= \frac{\gamma_{\rm A}}{2\pi} \left| \sum_{n=1}^{3} \frac{A_n}{{\rm i}\omega - x_n} \right|^2 \\ &\quad + \frac{\gamma_{\rm B}}{2\pi} \left| \sum_{n=1}^{3} \frac{(x_n + \kappa_{\rm a})\,(x_n + \kappa_{\rm b}) + g_{\rm A}^2}{g_{\rm A} g_{\rm B}} \frac{A_n}{i\omega - x_n} \right|^2. \end{aligned} \tag{9}$$

The other is the spectrum along the cavity axis, which corresponds to the autocorrelation of the cavity field and is given by

$$S_{\rm axis} = \frac{\kappa}{\pi} \left| \int_0^\infty {\rm d}t\,{\rm e}^{{\rm i}\omega t} c(t) \right|^2 = \left| \sum_{n=1}^{3} \frac{x_n + \kappa_{\rm a}}{g_{\rm A}} \frac{A_n}{{\rm i}\omega - x_n} \right|^2. \tag{10}$$

In Eqs. (8)–(10), the coupled system consisting of two QDs and a single-mode cavity has poles at x_n where the spontaneous emission peaks are expected. The coefficients of the exponential terms correspond to the amplitude of these peaks. The $S_{\rm side}$ is composed of two spontaneous emission terms originated from the two QDs, which are $a(t)$ and $b(t)$, while $S_{\rm axis}$ only includes the cavity mode term $c(t)$.

3. Results and discussions

The spontaneous emission spectrum for a two-level atom coupled to a cavity model has been fully understood.[1] In the strong-coupling limit, both the side and axis spectrum components, whose emission probabilities differ from each other, approach the so-called vacuum Rabi spectrum. In our model, we assume that the QD-cavity system is prepared in the single-quantum state, so that equation (5) can be solved within the four states $|2_{\rm A}\rangle\,|1_{\rm B}\rangle\,|0\rangle$, $|1_{\rm A}\rangle\,|2_{\rm B}\rangle\,|0\rangle$, $|1_{\rm A}\rangle\,|1_{\rm B}\rangle\,|1\rangle$, and $|1_{\rm A}\rangle\,|1_{\rm B}\rangle\,|0\rangle$. It should be noted that due to the damped cavity, this system has to end up in the steady state $|\psi_0\rangle = |1_{\rm A}\rangle\,|1_{\rm B}\rangle\,|0\rangle$ in the long-time limit of $t \to \infty$. For simplicity and without lose of generality, we let $\Delta_{\rm c} = 0$. The emission of a photon by the excited state of QD A is coherently reabsorbed by the cavity mode and QD B, and then the photon will be reemitted and reabsorbed a number of times before it eventually leaves the cavity.

For this strong coupling regime and high-Q PC cavity, the role of the decay parameters is almost negligible as the decay from QDs and leakage from the cavity is much smaller than the radiative coupling between the two QDs and cavity mode ($\gamma_j, \kappa \ll g_j$). For this reason, in the following calculations, we explicitly ignore the decay terms in Eqs. (5)–(10) in order to get simple analytical results for the spectra. By using the simplification, the origin of the interference effect becomes more transparent. Furthermore, by considering two general cases: the on-resonance case, where the transition frequencies of two QDs are equal to each other, and the off-resonance case, where the detuning between the two transition frequencies is not zero, one can explore the way to control the characteristics of the interference process during spontaneous emission. It turns out that they can be fully manipulated by the coupling strength g_j and the detuning between the transition frequencies of QD $\omega_{\rm AB}$ when the decay parameters are equal to each other ($\gamma_{\rm A}/2 = \gamma_{\rm B}/2 = \kappa$).

3.1. On-resonance case with the same transition frequencies

In the case of on-resonance excitation where ω_A=ω_B, the rigorous calculation results of the spectra from Eqs. (9) and (10) as a function of the detuning $\delta = \omega - \omega_c$ for different g_j are shown in Fig. 2: one for the spontaneous emission from the side of the system (the side spectrum S_{side}) and one for the spontaneous emission from the axis direction (the axis spectrum S_{axis}). The system is initially in the upper level of QD A. We find that S_{side} presents three peaks, one center peak and two symmetrical side peaks, and S_{axis} exhibits two peaks, which have equal heights and are symmetrically located in the two sides of the zero detuning.

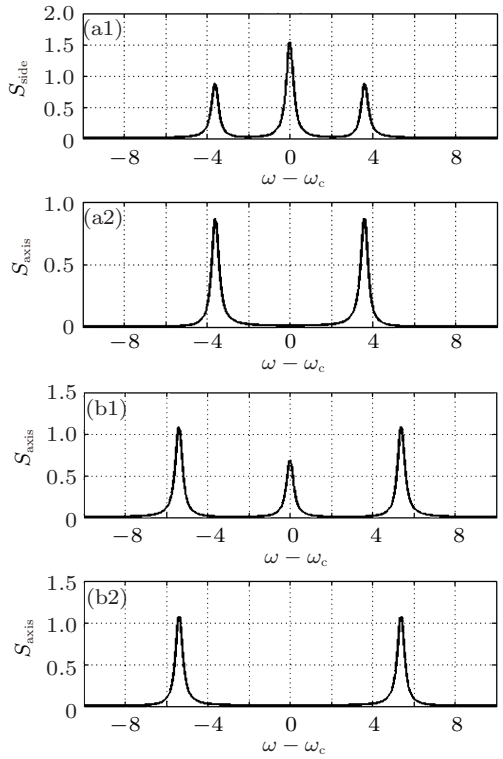


Fig. 2. Spontaneous emission spectrum as a function of detuning $\delta = \omega - \omega_c$ when $\omega_A = \omega_B = 100$. (a1) S_{side} and (a2) S_{axis} for $g_A = 3$, $g_B = 2$; (b1) S_{side} and (b2) S_{axis} for $g_A = 5$, $g_B = 2$. $\gamma_A/2 = \gamma_B/2 = \kappa = 0.2$ (in arbitrary units).

In the current case, we keep g_B =2 and change g_A from 3 to 5. We find that the distance between adjacent peaks increases as the coupling strength g_A is enhanced. The strength of the central peak in S_{side} decreases as g_A increases. The relative heights of the two side peaks in the emission spectra remain equal, and an increase in g_A will enhance their heights. The above analysis indicates that the coupling strengths g_j not only influence the splitting degree but also the intensity of the peaks in the spontaneous emission spectra. This feature can also be clearly visualized in Eqs. (11) and (12), which present the analytical form of eigenvalues x_n $(n = 1,2,3)$ as

$$x_1 = 0, \quad x_{2,3} = \pm i\Omega_1, \tag{11}$$

where $\Omega_1 = \sqrt{g_A^2 + g_B^2}$. The corresponding eigenstates are

$$\begin{aligned}
|\phi_1\rangle &= \cos\theta\,|2_A,1_B,0\rangle - \sin\theta\,|1_A,2_B,0\rangle,\\
|\phi_2\rangle &= -\frac{i}{\sqrt{2}}[\sin\theta\,|2_A,1_B,0\rangle\\
&\quad + \cos\theta\,|1_A,2_B,0\rangle + i\,|1_A,1_B,1\rangle],\\
|\phi_3\rangle &= -\frac{i}{\sqrt{2}}[\sin\theta\,|2_A,1_B,0\rangle\\
&\quad + \cos\theta\,|1_A,2_B,0\rangle - i\,|1_A,1_B,1\rangle].
\end{aligned} \tag{12}$$

Here, $\sin\theta = g_A/\Omega_1$ and $\cos\theta = g_B/\Omega_1$.

It is apparent that each energy eigenstate decays to the ground state via two output channels: the side-way channel, which can be described by the following transition operator:

$$\sigma_+^A = |\psi_0\rangle\left[\cos\theta\,\langle\phi_1| + \frac{i}{\sqrt{2}}\sin\theta\,(\langle\phi_2| + \langle\phi_3|)\right], \tag{13a}$$

and the axial channel which is described by the following transition operator:

$$\sigma_+^B = |\psi_0\rangle\left[-\sin\theta\,\langle\phi_1| + \frac{i}{\sqrt{2}}\cos\theta\,(\langle\phi_2| + \langle\phi_3|)\right]. \tag{13b}$$

Abundant physical information can be found from Eqs. (11)–(13) to help understand the emission spectrum features. The Rabi oscillation Ω_1 leads to a splitting of the emission spectrum into three spectrum lines predicted at $\delta = 0$, $\pm\Omega_1$. The large coupling strength results in a wider splitting, as indicated by Eq. (11). This can be well understood in the dressed-state picture, as described by Eqs. (12) and (13). The atomic system we consider can be regarded as three dressed states decaying to the common ground state. Three peaks in the spectra correspond to transitions from the three upper levels to the ground level, respectively. Equation (13b) shows that the spectrum from the axis is a doublet which can be associated with the transitions from the two dressed states $|\phi_{2,3}\rangle$ to the ground state $|\psi_0\rangle$.

While some approximations have been adopted, the model discussed above contains the essential physical features that we wish to emphasize in this paper. Let us look closely at the amplitudes of each state, which are

$$\begin{aligned}
a(t) &= \left[\left(\frac{g_A}{g_B}\right)^2 + 1\right]^{-1} + \frac{1}{2}\left[\left(\frac{g_B}{g_A}\right)^2 + 1\right]^{-1}\\
&\quad \times \left(e^{i\Omega_1 t} + e^{-i\Omega_1 t}\right),
\end{aligned} \tag{14a}$$

$$b(t) = \left(\frac{g_A}{g_B} + \frac{g_B}{g_A}\right)^{-1}\left[\frac{1}{2}\left(e^{i\Omega_1 t} + e^{-i\Omega_1 t}\right) - 1\right], \tag{14b}$$

$$c(t) = \left[2i\sqrt{1 + \left(\frac{g_B}{g_A}\right)^2}\right]^{-1}\left(e^{i\Omega_1 t} - e^{-i\Omega_1 t}\right). \tag{14c}$$

The emission line in the side spectrum S_{side} is split into three peaks: one peak is located at the frequency of the cavity mode, and two side peaks have equal heights and the maxima are symmetrically located at $\delta = \pm\Omega_1$. In S_{axis} two side peaks are split symmetrically around $\delta = 0$, as shown in Fig. 2.

Next, we explore the influence of the coupling strength parameters on the amplitude of each peak in the emission spectra derived from Eq. (14). The consistent calculation results are shown in Fig. 3, which indicates that the amplitude of the central peak in $S_{\rm side}$ is proportional to $g_{\rm B}$ and inversely proportional to $g_{\rm A}$. Meanwhile, the side peaks in $S_{\rm side}$ and $S_{\rm axis}$ increase with the increase in $g_{\rm A}$ and decrease as $g_{\rm B}$ increases more. The physical picture for the QD–cavity system is now quite clear and simple. In this resonance case, the two coupling constants are proportional to the splitting among the three peaks. The symmetrical property in the spontaneous emission spectrum cannot be destroyed by the asymmetrical coupling constants. More populations are uniformly distributed on the upper and lower levels of the dressed states due to the large coupling constants between the cavity and QD A, which is initially located in the excited state. The variation behavior of the central peak under the influence of this coupling is inversed to that for the side peaks. On the other hand, one can also find from Fig. 3 that the influence of the coupling between the cavity and QD B on the height of the central peak and side peaks is the inverse of that with QD A.

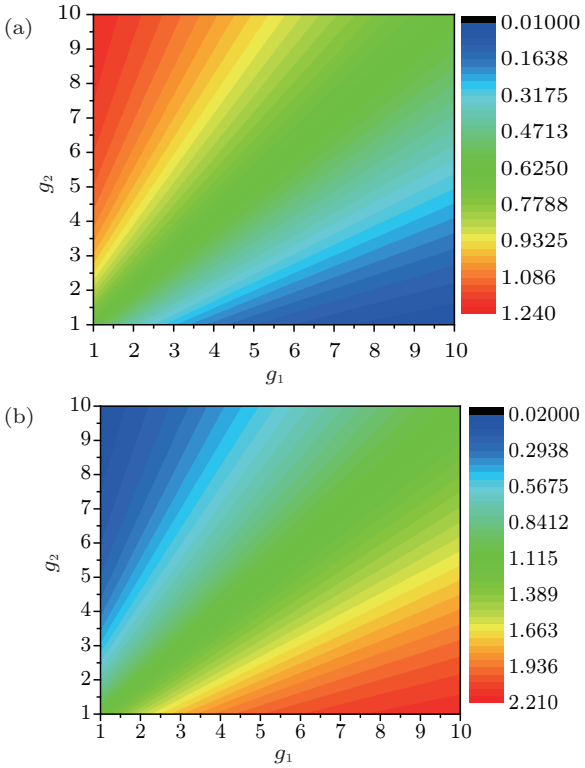


Fig. 3. (color online) Calculated heights of (a) middle and (b) side peaks as functions of the coupling strength g_j with $\omega_{\rm A} = \omega_{\rm B} = 100$ and $\gamma_{\rm A}/2 = \gamma_{\rm B}/2 = \kappa = 0.2$ (in arbitrary units) in the situation of $\gamma_j, \kappa \ll g_j$.

3.2. Off-resonance case with the same coupling constants

When the condition $g_{\rm A} = g_{\rm B} = g$ is satisfied in the off-resonance situation where $\omega_{\rm A} \neq \omega_{\rm B}$, the spontaneous emission spectrum can be controlled by the detuning between the transition frequencies of the two QDs, which is defined as $\omega_{\rm AB} = (\omega_{\rm A} - \omega_{\rm B})/2$. We have taken two groups of frequency parameters for the system with two detunings which are opposite to each other, and the details about the spontaneous emission spectrum variation are shown in Fig. 4. Unlike the resonance case in Fig. 2, both $S_{\rm side}$ and $S_{\rm axis}$ have three peaks and are no longer fully symmetric. The emission line is split symmetrically around the central peak which is located at the resonant frequency of the cavity mode, and the two side peaks do not continue to have the same peak height. The triplet peaks in $S_{\rm side}$ and $S_{\rm axis}$ are located at the same frequency. When $\omega_{\rm A} = 100$, $\omega_{\rm B} = 95$, as depicted in Fig. 4(a), the amplitudes of the three peaks are enhanced in turn as the detuning $\delta = \omega - \omega_{\rm c}$ increases. In Fig. 4(b), by exchanging the values of the two transition frequencies, the new spectrum is just the mirror inversion of Fig. 4(a), and there is no appreciable change in the frequency positions of the spectral lines.

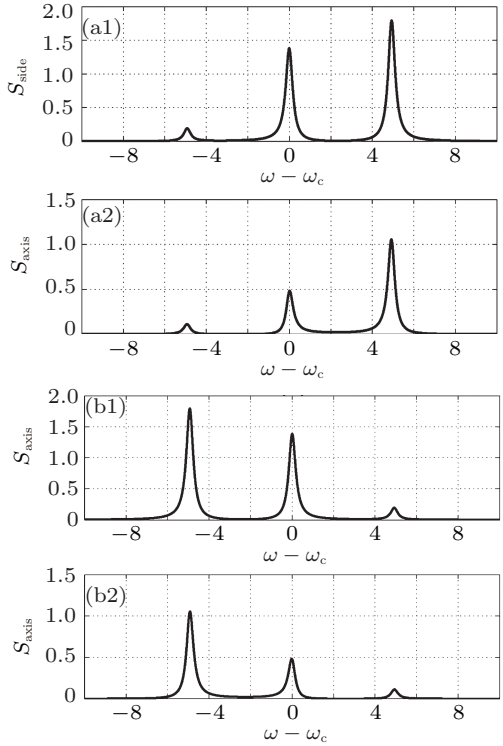


Fig. 4. Spontaneous emission spectrum as a function of detuning when $g_{\rm A} = g_{\rm B} = g = 2$. (a1) $S_{\rm side}$ and (a2) $S_{\rm axis}$ for $\omega_{\rm A} = 100$ and $\omega_{\rm B} = 95$; (b1) $S_{\rm side}$ and (b2) $S_{\rm axis}$ for $\omega_{\rm A} = 95$ and $\omega_{\rm B} = 100$. Other parameters are the same as those in Fig. 2.

The above features can also be found from the analytical solution of the coupled system. The eigenvalues of the evolution dynamics are now given by

$$x_1 = 0, \quad x_{2,3} = \pm {\rm i}\Omega_2, \tag{15}$$

where $\Omega_2 = \sqrt{\omega_{\rm AB}^2 + 2g^2}$. The eigenstates have the following form:

$$\begin{aligned} |\phi_{\rm a}\rangle &= \alpha\,|2_{\rm A}, 1_{\rm B}, 0\rangle - \alpha\,|1_{\rm A}, 2_{\rm B}, 0\rangle + \beta\,|1_{\rm A}, 1_{\rm B}, 1\rangle\,, \\ |\phi_{\rm b}\rangle &= \frac{1}{2}(1+\beta)\,|2_{\rm A}, 1_{\rm B}, 0\rangle \\ &\quad + \frac{1}{2}(1-\beta)\,|1_{\rm A}, 2_{\rm B}, 0\rangle + \alpha\,|1_{\rm A}, 1_{\rm B}, 1\rangle\,, \end{aligned}$$

$$|\phi_c\rangle = \frac{1}{2}(1-\beta)|2_A,1_B,0\rangle - \frac{1}{2}(1+\beta)|1_A,2_B,0\rangle - \alpha|1_A,1_B,1\rangle, \quad (16)$$

where $\alpha = 2ig/\Omega_2$ and $\beta = \omega_{AB}/\Omega_2$. To express it as we did for the resonant case, we can obtain the transition operator for the decay via the side pathway as

$$\sigma_+^A = |\psi_0\rangle\left[-\alpha\langle\phi_a| + \frac{1}{2}(1+\beta)\langle\phi_b| + \frac{1}{2}(1-\beta)\langle\phi_c|\right],$$
$$\sigma_+^B = |\psi_0\rangle\left[\alpha\langle\phi_a| + \frac{1}{2}(1-\beta)\langle\phi_b| + \frac{1}{2}(1+\beta)\langle\phi_c|\right], \quad (17a)$$

and the transition operator for the decay via the axial pathway as

$$a = |\psi_0\rangle\left[\beta\langle\phi_a| - \alpha(\langle\phi_b| - \langle\phi_c|)\right]. \quad (17b)$$

The amplitude of each state is given by

$$a(t) = \left(\frac{g}{\Omega_2}\right)^2 + \frac{1}{2}\left[1 + \frac{\omega_{AB}}{\Omega_2} - \left(\frac{g}{\Omega_2}\right)^2\right]e^{i\Omega_2 t} + \frac{1}{2}\left[1 - \frac{\omega_{AB}}{\Omega_2} - \left(\frac{g}{\Omega_2}\right)^2\right]e^{-i\Omega_2 t}, \quad (18a)$$

$$b(t) = \left(\frac{g}{\Omega_2}\right)^2\left[-1 + \frac{1}{2}\left(e^{i\Omega_2 t} + e^{-i\Omega_2 t}\right)\right], \quad (18b)$$

$$c(t) = \frac{ig}{\Omega_2^2}\left[-\omega_{AB} - \frac{1}{2}(\Omega_2 - \omega_{AB})e^{i\Omega_2 t} + \frac{1}{2}(\Omega_2 + \omega_{AB})e^{-i\Omega_2 t}\right]. \quad (18c)$$

From the eigenvalues given by Eq. (15), we consider the effects of the dynamical variables, namely, the Rabi frequencies, or more precisely the detuning between the two transition frequencies ω_{AB} on the spontaneous emission spectrum. The splitting peaks are more widely separated as ω_{AB} increases. This can be understood in the dressed state picture. From Eqs. (16) and (17), one can find that the three peaks in both spectra correspond to the transition from the three dressed states to the ground state. The two side peaks located at $\pm\Omega_2$ in each spectrum have unequal heights, which can be clearly visualized from Eq. (18). To contemplate some intuitive ideas about the dynamics of the quantum system, it is worth noting that equation (18) also tells us that the intensities of the two peaks change with the detuning parameter ω_{AB}, and the asymmetrical configuration is induced by the asymmetrical detuning parameters.

More detailed calculation results are displayed in Fig. 5, where no approximation is made. As ω_{AB} varies around zero detuning, the lines in Fig. 5 clearly show symmetrical properties, and these are responsible for the mirror relationship of the emission spectra between Figs. 4(a) and 4(b). Although the curves in Figs. 5(a) and 5(b) are similar to each other, they obey different regulations. As ω_{AB} varies from negative to positive, the height of the right side peak (blue line) monotonously grows and the left side peak (red line) decreases in S_{side}, and the change is sharp near the zero detuning. For a small value of the detuning parameter ω_{AB}, a larger population will be located on the dressed state $|\phi_a\rangle$ (black line) and then decay to the ground state. In the S_{axis} spectrum, the distribution of each peak illustrates a complicated and non-monotonous regulation with ω_{AB}. The maximum height of the left side peak (red line) appears when $\omega_A$is smaller than ω_B, while the right side peak (blue line) reaches its highest intensity when ω_A is larger than ω_B. In the S_{axis} spectrum, the black line describes the height of the central peak. Near the zero detuning, the black line displays a valley, and this can be attributed to the fact that the population is not distributed on the middle level of the dressed state. The central peak reaches its maximum height at some small detuning. The previous discussions clearly demonstrate that most of the physical information of the quantum coupled system is well reflected in the optical spectrum near zero detuning. When the two transition frequencies are far away from each other, namely, in the large detuning situation, the character of the spontaneous emission does not contain peculiar properties.

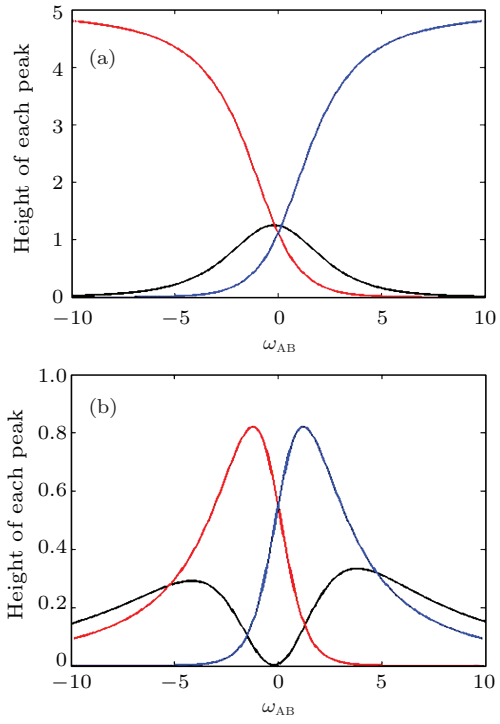


Fig. 5. (color online) Calculated heights of each peak in (a) S_{side} and (b) S_{axis} spectra as functions of ω_{AB} with $g_A = g_B = 2$. The black, red, and blue lines denote the height of the central peak, the left and right side peaks, respectively.

3.3. Effects of the atomic decay parameters

In this section, we present the strong coupling between two QDs and a single cavity mode in the situation of $\omega_A = \omega_B = \omega_c$ and $g_A = g_B = g$ to explore the influence of the decay parameters. When the two decay parameters are unequal to each other, namely, $\gamma_A/2 \neq \gamma_B/2$, singular feature (a peak or a dip) will appear at the frequency of the cavity mode in the

axis spectrum, which is presented in Fig. 6. However, there is no appreciable change in the shape and the position of the spectral line $S_{\rm side}$. When $\gamma_{\rm A} < \gamma_{\rm B}$, the singular feature presents as a small peak; and when $\gamma_{\rm A} > \gamma_{\rm B}$, it displays as a dip. After comparing the solid line and dashed line, decrease (increase) in the separation between the two decay parameters, the singular feature eventually becomes vanishing (obvious). In other words, the phenomenon is attributed to the unbalanced process of the emission and absorption of a single photon in the QD–cavity system. Anyway, the shape of the emitted spectrum line and especially the appearance of the singular feature in the middle of the $S_{\rm axis}$ spectrum are symptoms of the essential role played by quantum interference in this spontaneous decay process.

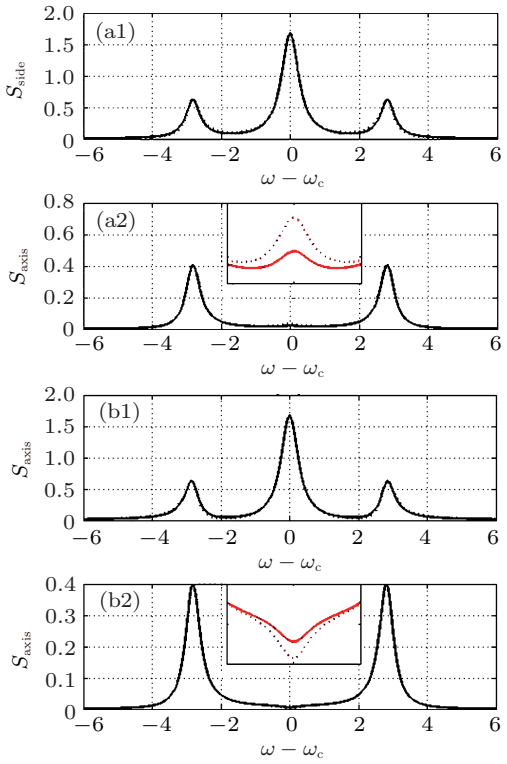


Fig. 6. (color online) Spontaneous emission spectrum as a function of the detuning when $\omega_{\rm A} = \omega_{\rm B}$. The two QDs have different atomic decay parameters under (a1) and (a2) the situation of $\gamma_{\rm A} < \gamma_{\rm B}$ ($\gamma_{\rm A}/2 = 0.2$, $\gamma_{\rm B}/2 = 0.4$ (solid line) and $\gamma_{\rm A}/2 = 0.1$, $\gamma_{\rm B}/2 = 0.5$ (dashed line)); (b1) and (b2) the situation of $\gamma_{\rm A} > \gamma_{\rm B}$ ($\gamma_{\rm A}/2 = 0.4\gamma_{\rm B}/2 = 0.2$ (solid line) and $\gamma_{\rm A}/2 = 0.5$, $\gamma_{\rm B}/2 = 0.1$ (dashed line)). The other parameters are $\kappa = 0.2$, $g = 2$, and $\omega_{\rm A} = \omega_{\rm B} = \omega_{\rm c} = 100$ (in arbitrary units). The two curves nearly overlap with each other. The inset shows the details of the singular feature, which shows a weak difference.

4. Conclusion

In summary, we have theoretically investigated the spontaneous emission spectrum of two QDs that are strongly coupled with a single-mode nanocavity. Emissions both from the side and along the axis of the cavity are considered. The quantum dynamics of the coupled system can be solved via a rigorous numerical approach, and a simple analytical form of solution can be achieved in some situations. On one hand, the spectrum strongly depends on the coupling strength g_j and the detuning between the two transition frequencies of the two QDs $\omega_{\rm AB}$, which can be studied in the dressed-state picture. When the QDs are at-resonance or off-resonance coupled with the cavity mode, different properties appear in the spontaneous emission spectrum.

In the on-resonance case of $\omega_{\rm A} = \omega_{\rm B}$, the $S_{\rm side}$ spectrum presents three peaks which have one central peak and two symmetrical side peaks, and $S_{\rm axis}$ spectrum exhibits two peaks which have equal heights symmetrically located on two sides of the zero detuning. The influence of the coupling strength g_j on the emission spectra has been explored in detail. Enhancement of g_j increases the splitting of the peaks in $S_{\rm side}$ and $S_{\rm axis}$. Moreover, the amplitude of the central peak is proportional to $g_{\rm B}$ and inversely proportional to $g_{\rm A}$. For the side peaks, the changes are opposite to the central one. In addition, the asymmetry in the coupling parameter does not affect the symmetrical character of the spectra.

In the case of off-resonance which satisfies the situations of $\omega_{\rm A} \neq \omega_{\rm B}$ and $g_{\rm A} = g_{\rm B}$, the detuning parameter $\omega_{\rm AB}$ will bring about a triple-peak asymmetric spectrum. In addition, the space between adjacent peaks grows larger as the detuning increases. We have carefully examined the relative heights of the three peaks and found that although the $S_{\rm side}$ and $S_{\rm axis}$ spectra are similar to each other, they obey different regulations, and most of the physical information is well reflected in the spectrum near zero detuning. When $\omega_{\rm AB}$ are opposite to each other, the spectra display a mirror relationship. It is the asymmetrical transition frequencies but not the asymmetric coupling strengths that determine the asymmetrical property of the spectra.

On the other hand, when the side and axis decay parameters differ from each other, a singular feature (a peak or dip) appears at the frequency of the cavity mode in the axial emission spectrum, and this is attributed to the unbalanced process of the emission and absorption of a single photon. In comparison, the side emission spectrum always exhibits a feature of triplet peaks. Our study can help to explore and sharpen the insightful understanding of the interaction of multiple quantum entities with photons in optical cavities.

References

[1] Carmichael H J 1999 *Statistical Methods in Quantum Optics* (vol. 1, 2) (Berlin: Springer)
[2] Boozer A D, Boca A, Miller R, Northup T E and Kimble H J 2007 *Phys. Rev. Lett.* **98** 193601
[3] Shen J T and Fan S H 2009 *Phys. Rev. A* **79** 023837
[4] Vahala K J 2003 *Nature* **424** 839
[5] Fidio C D and Vogel W 2009 *Phys. Rev. A* **79** 050303
[6] Song B S, Noda S, Asano T and Akahane Y 2005 *Nature Mater.* **4** 207
[7] Hennessy K, Badolato A, Winger M, Gerace D, Atature M, Gulde S, Falt S, Hu E L and Imamoglu A 2007 *Nature* **445** 896
[8] Nomura M, Kumagai N, Iwamoto S, Ota Y and Arakawa Y 2010 *Nature Phys.* **6** 279
[9] Li Z Y, Lin L L and Zhang Z Q 2000 *Phys. Rev. Lett.* **84** 4341
[10] Li Z Y and Xia Y N 2001 *Phys. Rev. A* **63** 043817

[11] Kouwenhoven L, Austing D G and Tarucha S 2001 *Rep. Prog. Phys.* **64** 701

[12] Mizubayashi J, Haruyama J, Takesue I, T Okazaki, Shinohara H, Harada Y and Awano Y 2008 *Microelectron. J.* **39** 222

[13] Garnier A A, Simon C, Gérard J M and Poizat J P 2007 *Phys. Rev. A* **75** 053823

[14] Gerace D, Türeci H E, Imamoglu A, Giovannetti V and Fazio R 2009 *Nature Phys.* **5** 281

[15] McKeever J, Boca A, Boozer A D, Buck J R and Kimble H J 2003 *Nature* **425** 268

[16] Painter O, Lee R K, Scherer A, Yariv A, O'Brien J D, Dapkus P D and Kim I 1999 *Science* **284** 1819

[17] Florescu L, John S, Quang T and Wang R Z 2004 *Phy. Rev. A* **69** 013816

[18] Cui G Q and Raymer M G 2006 *Phys. Rev. A* **73** 053807

[19] Hughes S and Yao P 2009 *Opt. Express* **17** 3322

[20] Gevaux D G, Bennett A J, Stevenson R M, Shields A J, Atkinson P, Griffiths J, Anderson D, Jones G A C and Ritchie D A 2006 *Appl. Rev. Lett.* **88** 131101

[21] Naesby A, Suhr T, Kristensen P T and Mork J 2008 *Phys. Rev. A* **78** 045802

[22] Auffeves A, Gerard J M and Poizat J P 2009 *Phys. Rev. A* **79** 053838

[23] Di Z, Jones H V, Dolan P R, Fairclough S M, Wincott M B, Fill J, Hughes G M and Smith J M 2012 *New J. Phys.* **14** 103048

[24] Midolo L, Pagliano F, Hoang T B, Xia T, van Otten F W M, Li L H, Linfield E H, Lermer M, Hofling S and Fiore A 2012 *Appl. Phys. Lett.* **101** 091106

[25] Gan Z S, Jia B H, Liu J F, Wang X H and Gu M 2012 *Appl. Phys. Lett.* **101** 071109

[26] Rao V S C M and Hughes S 2007 *Phys. Rev. Lett.* **99** 193901

[27] Laucht A, Gunthner T, Putz S, Saive R, Frederick S, Hauke N, Bichler M, Amann M C, Holleitner A W, Kaniber M and Finley J J 2012 *J. Appl. Phys.* **112** 093520

[28] Hughes S and Kamada H 2004 *Phys. Rev. B* **70** 195313

[29] Wu J, Lü X Q, Jin P, Meng X Q and Wang Z G 2011 *Chin. Phys. B* **20** 064202

[30] Wang X G, Feng M and Sanders B C 2003 *Phy. Rev. A* **67** 022302

[31] Zhang K and Li Z Y 2010 *Phys. Rev. A* **81** 033843

[32] Mckeever J, Buck J R, Boozer A D and Kimble H J 2004 *Phys. Rev. Lett.* **93** 143601

[33] Li G X, Tan H T, Wu S P and Yang Y P 2004 *Phys. Rev. A* **70** 034307

[34] Laussy F P, del Valle E and Tejedor C 2009 *Phys. Rev. B* **79** 235325

[35] Laucht A, Villas-Bôas J M, Stobbe S, Hauke N, Hofbauer F, Böhm G, Lodahl P, Amann M C, Kaniber M and Finley J J 2010 *Phys. Rev. B* **82** 075305

[36] Wang X X, Zhang J Q, Yu Y F and Zhang Z M 2011 *Chin. Phys. B* **20** 110306

[37] Yu T, Zhu A D and Zhang S 2012 *Chin. Phys. B* **21** 050304